Publishing House
AKAPIT

COMPUTER METHODS IN MATERIALS SCIENCE

Informatyka w Technologii Materiałów

Vol. 12, 2012, No. 2

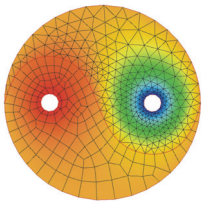

SELECTION OF THE APPROPRIATE PHASE TRANSFORMATION MODEL FOR DESIGN OF LAMINAR COOLING AND CONTINUOUS ANNEALING OF DP STEELS

DANUTA SZELIGA

AGH University of Science and Technology, al. Mickiewicza 30, 30-059 Kraków, Poland
Corresponding author: szeliga@agh.edu.pl

Abstract

In the work a modified JMAK phase transformation model dedicated to dual phase steels was proposed. The model was validated with sensitivity analysis methods and the most important model parameters were selected. The sensitivity analysis results were next used in the parameters identification task. That task was formulated as an inverse problem, which was transformed to the optimization task. The minimum of the goal function defined in the optimization problem was the solution of the model parameters identification. The phase transformation model outputs with identified parameters were compared to measurements from dilatometer and microsections analysis. The comparison confirmed good agreement between measurements and predictions. Two different case studies were defined to apply modified JMAK model to finite element software and to perform simulations of selected case studies. Investigated procedure proved applicability to modelling of complex industrial processes combining material forming and cooling/annealing.

Key words: phase transformation model, sensitivity analysis, parameters identification, laminar cooling and annealing modeling

1. INTRODUCTION

Large number of phase transformation models are available in the literature, from the simplest ones based on the JMAK equation (Avrami, 1939) through more advanced models based on phase field (Simmons et al., 2000) or solution of differential equation (Suehiro et al., 1992) to discrete models based on the Cellular Automata method (Lan et. al., 2004). All these models are characterised by various complexity of mathematical formulation and various predictive capabilities. Two aspects decide about accuracy and effectiveness of the phase transformation modelling:

- Selection of a relevant model for a particular application,
- Correct identification of models' parameters.

In metals processing the problem of identification of models using inverse analysis was widely investigated for flow stress models, see for example Author papers Szeliga et al. (2006), Szeliga and Pietrzyk (2010). Application of the inverse analysis to the identification of phase transformation models is presented in Pietrzyk et al. (2003), Kondek et al. (2003) and this approach is used in the present work.

Selection of the relevant phase transformation model for a particular application is the general objective of this paper. This selection has to be made by searching for a balance between model predictive capabilities and computing costs. A classification of the models with respect to the two mentioned criteria was made by Szeliga and Pietrzyk (2011) for metal forming processes. Making such a classification for the phase transformation models is the first

 ISSN 1641-8581

particular objective of the present paper. The following objectives compose selection of the model for applications connected with optimization of technological processes, performing the sensitivity analysis of the models and using this analysis to formulation of the most efficient version of the model. The case studies of the application of the selected model to industrial processes of the continuous annealing for dual phase (DP) steel are presented in the second part of the paper.

2. CLASSIFICATION OF PHASE TRANSFORMATION MODELS

Historically, JMAK type equations (Avrami, 1939; Kolmogorov, 1937; Johnson & Mehl, 1939) were commonly used for simulations of phase transformations. In this approach, all attention is focused on the kinetics and microstructural aspects are essentially ignored. However, even in the simplest JMAK model, nucleation and growth are recognized as being the two relevant and intrinsically different processes. The Avrami exponent is shown to be related to the nucleation conditions (Tamura et al., 1988), even though only two modes of nucleation kinetics are considered: site saturation and continuous nucleation at a constant rate. In the case of site saturation, all nuclei are present and active at the start of the transformation, and their number density remains constant during the entire transformation. In the case of continuous nucleation, the number of activated nucleation sites increases at a constant rate during the transformation, with a rate of nucleus formation depending on temperature and the fraction of parent phase still present. More advanced model was developed by Suehiro et al. (1992), who proposed differential equations describing kinetics of transformation separately for the continuous nucleation and the site saturation.

More refined transformation models incorporate relevant features of the parent microstructure. The simplest approach considered the austenite grain as a sphere and the ferrite to nucleate uniformly along the outer surface. In this simplified model, the final ferrite grain size is necessarily identical to the prior austenite grain size, and assuming ferrite growth to be controlled by carbon diffusion in austenite, provides a satisfactory description of austenite decomposition in most Fe-C alloys. However, more sophisticated growth parameters (i.e. interface mobility, solute-drag effect) have to be introduced as adjustable parameters to describe the growth rate of ferrite in more complex alloys, including Fe-C-Mn steels. Therefore, geometrically more-refined models, in which the austenite grain is assumed to be a more complex geometrical figures, were proposed (van Leeuwen et al., 1999). These approaches allow incorporation of the ferrite nucleation site density per austenite grain as a modelling parameter to reproduce the grain size, depending on the cooling conditions.

In recent years, the phase field approach has emerged as one of the most powerful methods for modelling many types of microstructure-evolution processes, including the austenite decomposition (Simmons et al., 2000; Mecozzi et al., 2008; Militzer, 2011). Detailed description of this method was presented by Mecozzi et al. (2008). Very briefly, the phase-field model treats a polycrystalline system, containing both bulk and boundary regions, in an integral manner. A set of continuous phase-field variables, each of them representing an individual grain of the system, are defined to have a constant value inside the grains and change continuously over a diffuse boundary. In this approach each phase-field parameter of a grain is equal to 1 inside the grain and 0 elsewhere. At the interface between two grains there is a gradual change of the two corresponding phase field parameters from 0 to 1 such that the sum of all phase-field parameters holds 1 at each time step and at each point in the simulation domain. Following the formation of new (ferritic) nuclei in specific locations, depending on the cooling conditions, the microstructural evolution during the austenite to ferrite transformation is governed by the phase-field equations. The interfaces mobility, interfacial energies and the driving pressure for the transformation are parameters of these equations and they determine the kinetics of the austenite decomposition. The driving pressure is calculated from the local carbon composition within the diffuse interface, controlled by the carbon diffusion within the austenite. Therefore, the phase-field model describes the ferrite growth via a mixed-mode approach, i.e., both the carbon diffusion and the apparent mobility of the austenite/ferrite interface are accounted for.

Since early 1970-ies, finite element (FE) method has become the most popular simulation technique (Zienkiewicz & Taylor, 1989). In modelling phase transformations this method was applied to simulations of carbon distribution in austenite and became an alternative for the phase field models. Example of contribution to this research was presented by Pernach and Pietrzyk (2008). FE solution of the diffu-

sion equation with a moving boundary (Stefan problem) was performed in that work for various shapes of austenite and ferrite grains.

In the late 1990-ies such discrete methods as cellular automata (CA), molecular dynamics (MD) or Monte Carlo (MC) begun to be applied to modelling recrystallization and phase transformations during materials processing. The general idea of the CA model was presented by Zhang et al. (2003) and by Lan et al. (2004).

Classification of phase transformation models with respect to predictive capabilities and computing costs is presented in figure 1. The first group (bottom left corner in figure 1) contains models commonly used for fast simulations of industrial processes and they are generally limited to description of the kinetics of transformations and volume fractions of phases. Additivity rule (Scheil, 1935) has to be applied in these models to account for the temperature changes during transformations. In the second group (the centre in figure 1) there are differential equations or phase field technique models, usually applied to technology design and optimization of processes. These models accurately describe transformations in varying temperatures. The next group (further right in figure 1) includes models based on the FE solution of the diffusion equation with moving boundary (Pernach & Pietrzyk, 2008). Beyond the mentioned earlier parameters, these models are capable to predict distribution of carbon concentration in austenite and resulting hardness of bainite and martensite.

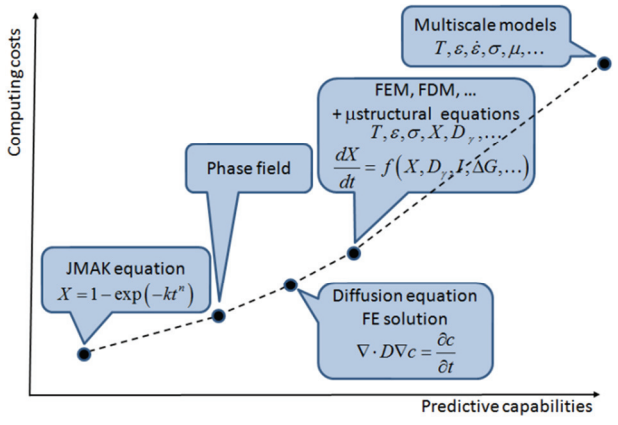

Fig 1. *Classification of selected phase transformation models: computing costs versus predictive capabilities.*

Significant extension of the predictive capabilities is obtained when mentioned earlier models are implemented into the finite difference or finite element codes, which simulate industrial thermomechanical processes (Pietrzyk & Kuziak, 1999). This coupling involves increase of the computing costs. Finally, the most advanced models (the top right corner in figure 1) connect FE codes with discrete models such as Cellular Automata (CA), Molecular Dynamics (MD) or Monte Carlo (MC). Combining of FE code and CE model, called CAFE approach, seems to be the most frequently used. New quality of information concerning microstructural features during phase transformations is obtained from these models but the increase of the computing costs is significant.

Performed analysis of the phase transformation models and published data (Bhadeshia, 2001) lead to the conclusion that the modified JMAK equation models are accurate and efficient enough to be applied in the optimization tasks, when volume fractions of phases are the optimization parameters. Since the objective of the present work is fast prediction of transformation temperatures and volume fractions of structural components in industrial processes, the modifications of this equation are considered in the next sections.

3. MODIFIED JMAK MODEL

3.1. Model description

The general form of the JMAK equation is:

$$X = 1 - \exp\left(-kt^n\right) \tag{1}$$

where: X – transformed volume fraction, k, n – coefficients.

Theoretical considerations show that, according to transformation type (nucleation and growth process, site saturation process) a constant value of coefficient n in equation (1) can be used. The values of n are introduced in the model as a_4, a_{15} and a_{24} for ferritic, pearlitic and bainitic transformations, respectively. Coefficient k should map the form of a TTT diagram. Following that observation, the k is defined as a temperature function $k = f(T)$. Various forms of k were tested in the present work. Too simple function may cause low accuracy of the model and too complex function may cause problems with the identification of the model and lack of the uniqueness solution. The function $k = f(T)$ has to be flexible enough to replicate complex phenomena of nucleation and growth controlled by diffusion, interface mobility and solute-drag effect. These phenomena are reversibly dependent on the temperature. Rate of nucleation increases with the temperature drop below Ae_3. Contrary, diffusion becomes slower

at lower temperatures. That inspired Donnay et al. (1996) to propose a modified Gaussian function for parameter k, which is used for ferritic transformation in this work:

$$k = k_{\max} \exp\left[-\left(\frac{T - T_{nose}}{a_7} \right)^{a_8} \right] \tag{2}$$

The four coefficients in this function k_{max}, T_{nose}, a_7, a_8 allow to describe all shapes of the TTT curves in a quite intuitive way: k_{max} is the maximum value of k, T_{nose} is a temperature position of the nose of the Gaussian function and represents the temperature of the maximum rate of the transformation, a_8 is proportional to the nose width at mid height and a_7 is related to the sharpness of the curve.

Equation (2) is supposed to account for the influence of the austenite grain size at the beginning of the transformation. Thus, the following equations are used to calculate coefficients k_{max} and T_{nose}:

$$k_{\max} = \frac{a_5}{D_\gamma} \tag{3}$$

$$T_{nose} = Ae_3 + \frac{400}{D_\gamma} - a_6 \tag{4}$$

where: D_γ – austenite grain size at the beginning of transformation.

It was concluded from the primary model investigations that there is no need to introduce such a complex function $k(T)$ for pearlitic and bainitic transformations. Therefore, a slightly simpler function was selected for the pearlitic transformation:

$$k = \frac{a_{14}}{D_\gamma^{a_{16}}} \exp\left(a_{13} - \frac{a_{12} T}{100} \right) \tag{5}$$

In the bainitic transformation the dependence on the grain size D_γ is neglected:

$$k = a_{23} \exp\left(a_{22} - \frac{a_{21} T}{100} \right) \tag{6}$$

In the model phases incubation times should be accounted for. Equation (1) combined with function (2) do not require the incubation time. It is assumed that ferritic transformation begins when the volume fraction of ferrite achieves 5%. Incubation times of the remaining transformations (τ_p, τ_b) are calculated as:

pearlite: $$\tau_P = \frac{a_9}{\left(\mathrm{Ae}_1 - T \right)^{a_{11}}} \exp\left[\frac{a_{10} \times 10^3}{R\left(T + 273 \right)} \right] \tag{7}$$

bainite: $$\tau_b = \frac{a_{17}}{\left(a_{20} - T \right)^{a_{19}}} \exp\left[\frac{a_{18} \times 10^3}{R\left(T + 273 \right)} \right] \tag{8}$$

Additional relationships in the model and equilibrium carbon concentrations are presented in table 1. Equilibrium concentrations $c_{\gamma\alpha}$ and $c_{\gamma\beta}$, as well as carbon content in the ferrite c_α, are introduced as temperature functions. These functions are polynomials and they are determined using ThermoCalc software based on the information on the steel chemical composition.

Table 1. *Additional equations in the model.*

$c_\gamma = \dfrac{\left(c_0 - X_f c_\alpha \right)}{1 - X_f}$	$X_{f0} = \dfrac{c_{\gamma\alpha} - c_0}{c_{\gamma\alpha} - c_\alpha}$
$c_{\gamma\alpha} = c_{\gamma\alpha 0} + c_{\gamma\alpha 1} T$, $c_{\gamma\beta} = c_{\gamma\beta 0} + c_{\gamma\beta 1} T$, $c_\alpha = f\left(T \right)$	

Notation: c_γ – average carbon content in the austenite, c_α – carbon content in the ferrite, c_0 – carbon content in the steel, $c_{\gamma\alpha}$ – carbon concentration in the austenite at the γ-α boundary, $c_{\gamma\beta}$ – carbon concentration in austenite at the γ-cementite boundary, X_{f0} – equilibrium (maximum) ferrite volume fraction in steel in a considered temperature.

Modelling of phase transformations starts with equation (1) when the temperature drops below Ae_3. The additivity rule (Scheil, 1935) is applied to the model to account for the temperature variations during transformation. The transformed ferrite volume fraction $X_f\left(T^i \right)$ is calculated with respect to the maximum volume fraction of ferrite $X_{f0}\left(T^i \right)$ for the temperature T^i. Thus, the volume fraction of ferrite with respect to the whole volume of the material is $F_f = X_{f0} X_f$ for the fixed temperature T^i. The value of X_f calculated from equation (1) for the varying temperature has to be corrected due to change of the equilibrium (maximum) ferrite volume fraction X_{f0}, which is the temperature function (see table 1):

$$X_f\left(T^{i+1} \right) = X_f\left(T^i \right) \frac{X_{f0}\left(T^i \right)}{X_{f0}\left(T^{i+1} \right)} \tag{9}$$

where: i – iteration number, T^i – temperature in i^{th} iteration.

Simulation continues until the transformed volume fraction achieves 1. However, when carbon content in austenite exceeds the limiting value $c_{\gamma\beta}$ (see table 1), the austenite-pearlite transformation begins in the remaining volume of the austenite.

Bainite start temperature T_{bs} and martensite start temperature T_{ms} are functions of the chemical composition of the austenite:

$$T_{bs} = a_{20} - 425[\mathrm{C}] - 42.5[\mathrm{Mn}] - 31.5[\mathrm{Ni}] \quad (10)$$

$$T_{ms} = a_{26} - a_{27} c_{\gamma} \quad (11)$$

Fraction of the austenite, which transforms into the martensite, is calculated according to the model of Koistinen and Marburger (1959), described also in Umemoto et al. (1992), Pietrzyk et al. (2003):

$$X_m = 1 - \exp\left[-0.011\left(T_{ms} - T\right)\right] \quad (12)$$

Equation (12) represents volume fraction of martensite with respect to the volume of austenite, which was remaining at the temperature T_{ms}. The volume fraction of martensite with respect to the whole volume of the material is:

$$F_m = \left(1 - F_f - F_p - F_b\right) X_m \quad (13)$$

where: F_f, F_p, F_b – volume fractions of ferrite, pearlite and bainite with respect to the whole volume of the sample.

Since continuous annealing was selected as a case study in the present work, transformation of the ferritic-pearlitic microstructure into the austenite has to be also considered. Kinetics of the austenitic transformation during heating is described by equation (1) with the coefficient $n = a_{30}$ and the coefficient k defined as:

$$k = a_{28} \exp\left[\frac{-a_{29} \times 10^{-3}}{R\left(T + 273\right)}\right] \quad (14)$$

Incubation time for the ferrite-austenite transformation is calculated from the equation:

$$\tau_a = \frac{a_1}{\left(T - \mathrm{Ae}_1\right)^{a_3}} \exp\left[\frac{a_2 \times 10^3}{R\left(T + 273\right)}\right] \quad (15)$$

Phase transformation model described by equations (1) – (15) was applied to predict the phases distribution in the material for two case studies processes: cooling with various cooling rates after multi step hot forming and continuous annealing after cold rolling. To perform the processes simulations the model was validated with sensitivity analysis first and next identified using inverse problem formulation (chapters 2.2 and 2.3). The results and comparison to physical simulations of these processes are presented in chapter 3.

3.2. Sensitivity analysis of the phase transformation model

Sensitivity methods. Model of austenite decomposition during cooling described in section 2.1 was validated with respect to the phase transformation model parameters $\mathbf{a} = \{a_4, \ldots, a_{27}, D_\gamma\}$ during cooling process. Sensitivity analysis (SA) methods were applied to estimate the effect of model parameters on model outputs and to evaluate possibility of simplification of model equations. SA allows to assess the accuracy of an analyzed object or process model. It determines the parameters contributing the most to the output variability. It also indicates the parameters that are insignificant and that may be eliminated from the model. Moreover, the sensitivity analysis evaluates the parameters, which interact with each other and determines the input parameters region for subsequent calibration space. Performing SA requires to define the following terms (Kleiber et al.; 1997, Szeliga, 2011):

- *Model outputs measure*. The measure expresses the model outputs as a scalar value.
- *Selection of the parameter domain points*. Design of experiment techniques to be used to select the lower number of points guaranteeing searching the whole parameters domain.
- *Sensitivity measure*. The sensitivities, defined as global indices or local ones, are estimated based on the model outputs measure variations caused by the model parameters changes.

Following Szeliga (2012a), in this work the sensitivity analysis was applied to evaluate the influence of the phase transformation model parameters on the model outputs. In consequence, the model was better investigated and its calibration and modification became possible. Three algorithms of the SA were applied. The first one, Morris (1991) Design (MD) that is a screening technique, gives qualitatively information on the model response sensitivity to the parameters. The two latter algorithms, McKay (1995) and Sobol' (1993), are based on estimation of correlation ratio and they provide quantitative information on model sensitivities to parameters variations. Description of all applied methods is presented below.

Morris Design. Morris one-at-a-time Design belongs to the group of screening methods. In the algorithm the elementary effect ξ_i is introduced to calculate the sensitivities:

$$\xi_i(\mathbf{x}) := \frac{y(x_1,\ldots,x_{i-1},x_i+\Delta_i,x_{i+1},\ldots,x_k)-y(\mathbf{x})}{\Delta_i} \tag{16}$$

where: y is the model output, $\mathbf{x} \in \Omega \subset \mathrm{R}^k$ is the k-dimensional vector of model parameters x_i. The assumption is made that components x_i, $i = 1 \ldots k$, accept values of $\langle 0,1 \rangle$ interval, Δ_i is the i^{th} parameter disturbance.

A finite distribution F_i of elementary effects ξ_i calculated for the i^{th} factor is found by sampling $\mathbf{x}$ in Ω. Based on the distribution F_i, expected value μ_i and standard deviation σ_i for i^{th} model parameter are estimated through the classic estimators for independent random samples. Since the calculations of elementary effects ξ_i are sensitive to the parameter disturbance Δ_i, finite distribution F_i is estimated with various values of Δ_i. To compare the results of means μ_i and standard deviations σ_i estimations obtained for various Δ_i, μ_i and σ_i are normalized:

$$\mu_i^* = \frac{\mu_i}{\|\boldsymbol{\mu}\|} \qquad \sigma_i^* = \frac{\sigma_i}{\|\boldsymbol{\sigma}\|} \tag{17}$$

where $\boldsymbol{\mu} = (\mu_1,\ldots,\mu_k)$, $\boldsymbol{\sigma} = (\sigma_1,\ldots,\sigma_k)$.

The higher expected value of the parameter elementary effect is, the higher sensitivity of the model output with respect to that parameter is observed. The high value of the standard deviation means that either the parameter impact on the model output is nonlinear or the parameter interacts with other model parameters.

Two latter algorithms originate from probability theory. The first one assumes that the model output $y = y(\mathbf{x})$, $\mathbf{x}$ – parameters input vector, is given by the conditional expectation E of the random variable Y conditioned on model inputs $\mathbf{x}$: $y = E(Y \mid \mathbf{x})$. Thus, the prediction variance $Var(Y)$ can be expressed as:

$$Var(Y) = Var_{\mathbf{X}}\left(E(Y \mid \mathbf{x})\right) + E_{\mathbf{X}}\left(Var(Y \mid \mathbf{x})\right) \tag{18}$$

The first component of equation (18) is called Variance of Conditional Expectation $VCE(X_i)$, the second one is the residual part. The variation in y and by implication the variation of $E(Y \mid \mathbf{X} = \mathbf{x})$ as $\mathbf{x}$ varies, is measured by VCE. The second term in equation (18) is the error or residual term including the remaining variability in y caused by unobserved inputs or sources of variations when $\mathbf{x}$ is fixed. Thus the sensitivity index, called correlation ratio η^2 is defined as the ratio of $VCE(X_i)$ magnitude to prediction variance:

$$\eta^2 = \frac{Var_{\mathbf{X}}\left(E(Y|\mathbf{x})\right)}{Var(Y)} \cong \frac{VCE(X_i)}{\overline{Var}(Y)} \tag{19}$$

To calculate sensitivity index η^2 estimators for $VCE(X_i)$ and $\overline{Var}(Y)$ are needed. McKay (1995) method was used in this work. McKay proposed that the estimators are derived from Analysis of Variance and the sampling plan is based on Latin Hypercube Sampling (LHS), McKay (1979).

The second variance based method used in this work is Sobol' (1993) algorithm. The main assumption of the procedure are presented below:

1. Input k-parameters space Ω^k is a k-dimensional unit cube $\Omega^k = \{\mathbf{x} : 0 \le x_i \le 1, i = 1..k\}$.
2. The model function $y(\mathbf{x})$ is decomposed into sum of increasing dimensionality components:

$$y(\mathbf{x}) = y_0 + \sum_{i=1}^{k} y_i(x_i) + \sum_{1\le i<j\le k} y_{ij}(x_i,x_j) + \ldots + y_{1,\ldots,k}(x_1,\ldots,x_k) \tag{20}$$

3. Sobol' proved that the decomposition is unique and all the components can be evaluated by integrals, especially:

$$y_0 = \int_{\Omega^k} y(\mathbf{x})\,d\mathbf{x}, \quad y_i(x_i) = -y_0 + \int_0^1 \ldots \int_0^1 y(\mathbf{x})\,d\mathbf{x}_{\sim i} \tag{21}$$

where $d\mathbf{x}_{\sim i}$ denotes integration over all parameters except x_i. The integrals are estimated using Monte Carlo method.

Thus, the total variance $\overline{Var}(Y)$ is defined as:

$$\overline{Var}(Y) = \int_{\Omega^k} y^2(\mathbf{x})\,d\mathbf{x} - y_0^2 \tag{22}$$

And the variance of conditional expectation $VCE(X_i)$ is computed as:

$$VCE(X_i) = \int_0^1 y_i^2(x_i)\,dx_i \tag{23}$$

From equations (22) and (23) and taking equation (19), the sensitivity measure, called the first order Sobol' sensitivity index S_i, is estimated.

Sensitivity calculations. Sensitivity of the modified JMAK phase transformation model with respect to the model parameters was estimated using three presented above methods. The model inputs were: $\mathbf{x} = \{cr, \mathbf{a}\}$, where cr – cooling rate, $\mathbf{a} = (a_4, \ldots, a_{27}, D_\gamma)$ – parameters of the JMAK model for cooling process. Ten model outputs $y = (T_{ij}, X_i)$ were analyzed, where T – temperature, X_i – phase volume fraction, $i \in \{f, p, b, m\}$ indicates ferrite, pearlite, bainite or martensite phase, $j \in \{s, e\}$ indicates start/end of phase transformation, respectively. The modified JMAK model includes information on steel chemical composition as well as information on phases equilibrium conditions. Hence, the model validation was performed for the same dual phase steel which was used in the case studies presented in chapter 3. The chemical composition of the steel is listed in table 2 while the parameters describing carbon concentrations equilibrium, determined with ThermoCalc software, are provided in table 3.

The sensitivity results for all parameters $\mathbf{a} = \{a_4, \ldots, a_{27}, D_\gamma\}$ obtained for the investigated steel by Morris Design are presented in figure 2. It is observed that some of the model parameters do not impact any model outputs, some of them influence the model outputs in negligible way. These parameters cannot be identified based on analyzed model outputs and/or they should be eliminated from the model.

Extensive conclusions from the sensitivity analysis for the modified JMAK phase transformation model are given by Szeliga (2012b). Although in that paper the sensitivity calculations were carried out for the dual phase steel of different chemical composition, the conclusions are close to the present results. The conclusions are formulated as the summary results from application of all three sensitivity methods: Morris Design, Variance Analysis and Sobol' algorithm:

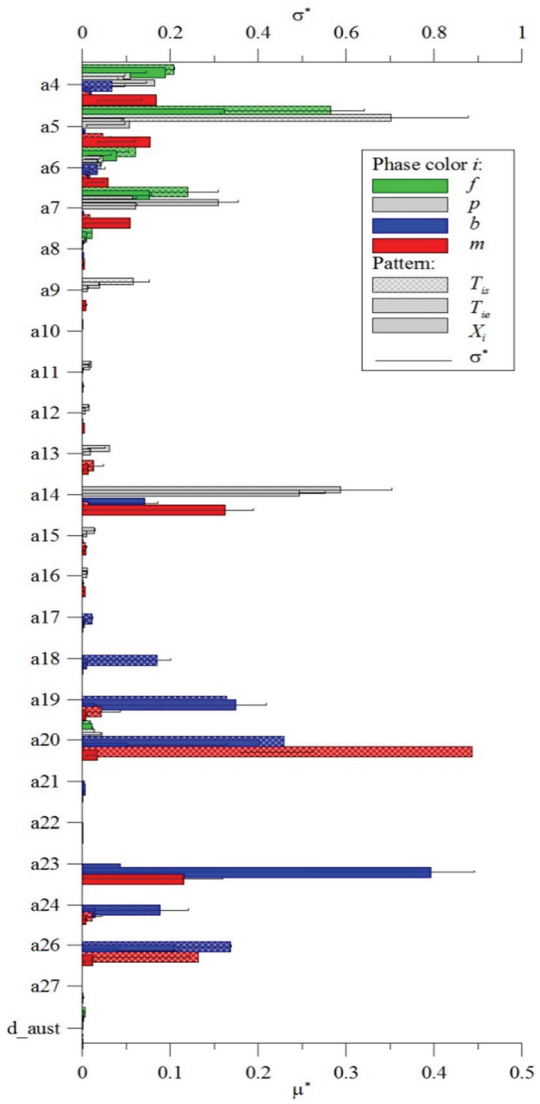

Fig. 2*. Sensitivity analysis results obtained by Morris Design for modified JMAK model of cooling process.*

– *Ferrite*. The results for ferrite transformation obtained from all sensitivity methods are presented in figure 3. Start temperature of ferrite transformation is the most sensitive to a_7 (parameter in k eq. (2)) – high impact of this parameter on T_{fs} and X_f is observed. Following remarks are made for the next parameters: a_4 (exponent in eq. (1)) – slight sensitivity to the temperature start T_{fs}, higher sensitivity to the volume fraction X_f, a_5 (parameter in k_{max} eq. (3)) and a_6 (parameter in T_{nose} eq. (4)) – both outputs: T_{fs} and X_f are sensitive to these parameters, a_8 (parameter in k eq. (2)) – low impact of this parameter on T_{fs} and X_f , a_{20} (parameter in T_{bs} eq. (10) and bainite incubation time τ_b in eq. (8)) – it determines T_{bs} and it indirectly influences X_f – thus

Table 2. *Chemical composition of the investigated steel, wght %.*

C	Mn	Si	P	S	Cr	Mo	Cu	Al	V	Nb	Ti	N
0.071	1.45	0.25	0.01	0.006	0.55	0.03	0.02	0.022	0.005	0.005	0.002	0.0039

Table 3. *Parameters in equations describing carbon concentrations equilibrium in table 1.*

$c_{\gamma\alpha 0}$	$c_{\gamma\alpha 1}$	$c_{\gamma\beta 0}$	$c_{\gamma\beta 1}$
4.8513	-0.005776	-1.46583	0.002887
$c_\alpha = -0.069 + 0.000435T - 9.1658\times10^{-7}T^2 + 6.487\times10^{-10}T^3$ for $T < 637^\circ$ C			
$c_\alpha = -0.0487268 + 0.00017839T - 1.50788\times10^{-7}T^2$ for $T > 637^\circ$ C			

higher sensitivity to X_f , low sensitivity to T_{fs} D_γ (parameter in k_{max} eq. (3)) – the same sensitivity conclusions as for a_{20}. Suggestion: parameter a_8 can be eliminated in modeling ferrite phase transformation. The lack of the model sensitivity on D_γ parameter is questionable. It should be pointed out that the dilatometric tests were performed only for one austenite grain size, thus dependence of the transformation kinetics on D_γ is not reliable. This problem should be further investigated by performing dilatometric tests for various grain size.

– *Pearlite*. For the considered chemical composition of steel the contribution of pearlite transformation is negligible and observed for low cooling rates, below 1°C/s. The conclusions on model sensitivity are formulated based on Morris Design calculations– figure 2. The start phase transformation temperature T_{ps} is sensitive to a_5 parameter in k_{max} eq. (3) for ferrite transformation, which indirectly impacts on the beginning of the pearlite transformation. The end phase transformation temperature T_{pe} and phase volume fraction X_p are sensitive first of all to a_{14} parameter in k eq. (5) for pearlite. Some sensitivity is observed for parameters a_4 and a_7 dedicated ferrite phase. For dual phase steel that was chosen for analysis those parameters determine if the pearlite transformation starts, hence their impact on the pearlite model outputs. The perlite transformation for dual phase steels is observed only for low cooling rates (lower than 1°C/s). Regarding that fact the model of the perlite transformation for DP steels can be simplified.

– *Bainite*. The results for bainite transformation obtained from all sensitivity methods are presented in figure 4. Three bainite phase model outputs: phase transformation temperature start/end T_{bs}/T_{be} and phase volume fraction X_b are sensitive to a_{20} parameter from T_{ms} eq. (10) and bainite k eq. (8) and next to a_{26} parameter from eq. (11) defining phase start temperature of martensite. Next T_{bs} is sensitive to a_{19} and a_{18} – parameters from bainite incubation time τ_b (eq.(8)). Lower sensitivity to these parameters is observed for T_{be}. The model output T_{be} is sensitive to a_{24}, which is the exponent n in eq. (1)). Latter parameters defining bainite transformation: a_{17}, a_{21}, a_{22}, a_{23} do not impact the bainite model outputs or their impact is very low. Suggestion: the bainitic transformation model can be simplified.

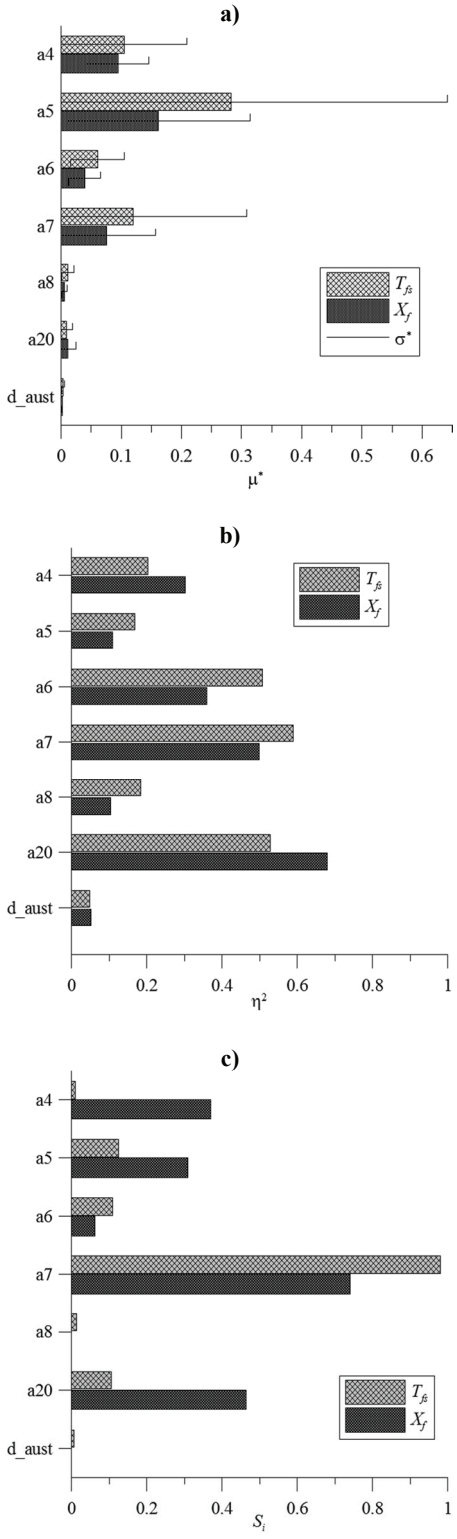

Fig. 3. *Ferrite phase sensitivity indices calculated with respect to parameters of modified JMAK model estimated by methods: a) Morris Design, b) Analysis of Variance, c) Sobol'.*

– *Martensite*. The results for martensite transformation obtained from all sensitivity methods are presented in figure 5. Phase temperature start T_{ms} is sensitive to a_{20} parameter from T_{bs} eq. (10) and next to a_{26} parameter from T_{ms} eq. (11). The results for phase volume fraction X_m are not consistent but the impact of listed above parameters

a_{20} and a_{26} is observed. Moreover slight influence of $a_4 - a_7$, a_{14} and a_{23} is noticed. Suggestion: parameter a_{27} from eq. (11) should not be modeled.

Summarizing, the sensitivity analysis indicated the set of parameters of the highest impact on the model outputs and in the parameters identification process they should be determined. The parameters of the low impact should be fixed or, if it is possible, eliminated from the model for dual phase steels.

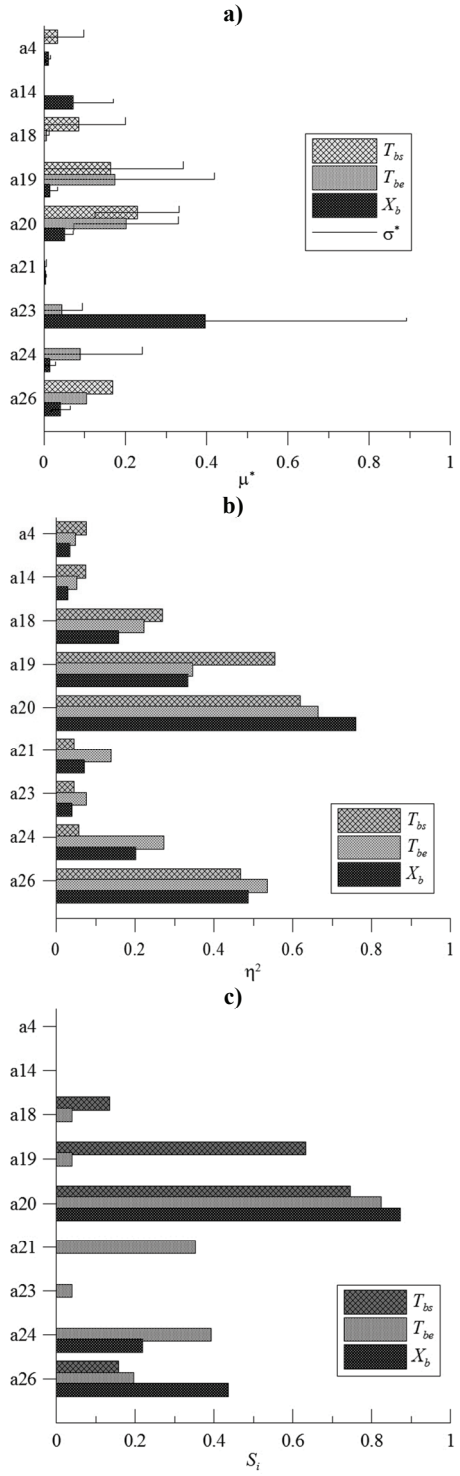

Fig. 4. *Bainite phase sensitivity indices calculated with respect to parameters of modified JMAK model estimated by methods: a) Morris Design, b) Analysis of Variance, c) Sobol'.*

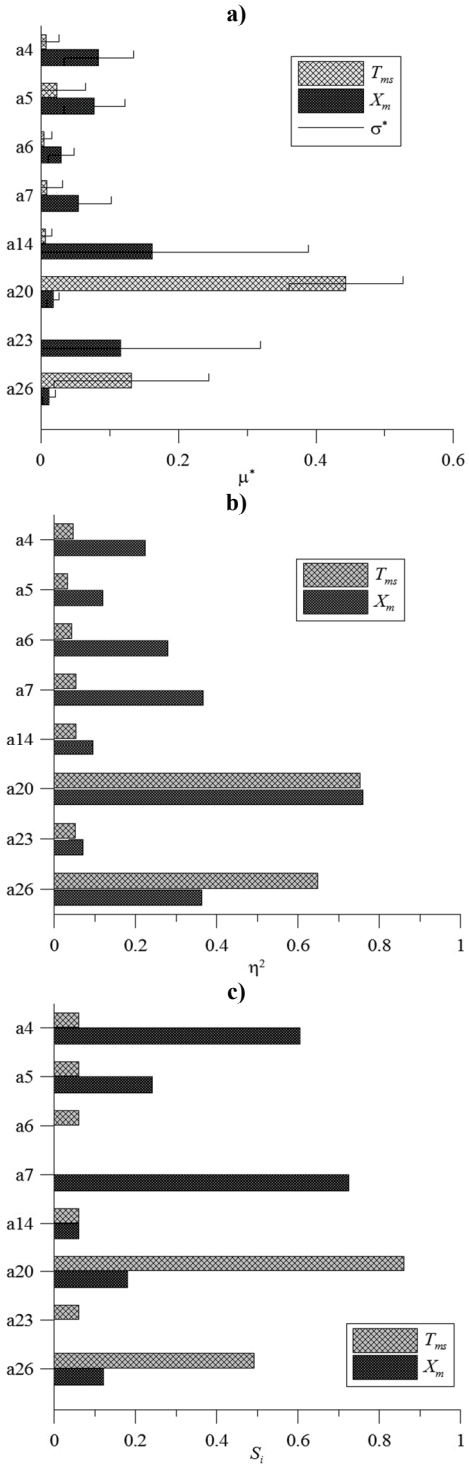

Fig. 5. *Martensite phase sensitivity indices calculated with respect to parameters of modified JMAK model estimated by methods: a) Morris Design, b) Analysis of Variance, c) Sobol'.*

3.3. Parameters JMAK model identification

Based on the results of model validation presented in section 2.2, the model was simplified and the parameters were identified. Simplification involved removing equation (5) with coefficients a_{12}, a_{13}, a_{14} and a_{16}. The constant coefficient $k = a_{12}$ was introduced for the pearlitic transformation. The identification task is formulated as an inverse one. The

modified JMAK model described in section 2.1 is the set of equations of the following form:

$$\mathbf{y} = f(\mathbf{x}) \tag{24}$$

where $\mathbf{y}$ is the vector of model outputs, $\mathbf{x} = (\mathbf{a}, \tilde{\mathbf{x}})$ is the vector of model inputs $\tilde{\mathbf{x}}$ (e.g. cooling rate) and model parameters $\mathbf{a}$.

The problem of parameters $\mathbf{a}$ identification, if model outputs $\mathbf{y}$ and inputs $\tilde{\mathbf{x}}$ are known, is called an inverse one:

$$\mathbf{y}, \tilde{\mathbf{x}}, f \quad \text{known} \quad \rightarrow \quad \text{estimate } \mathbf{a} \tag{25}$$

Estimation of the vector $\mathbf{a}$ requires information of model outputs $\mathbf{y}$ and model inputs $\tilde{\mathbf{x}}$. The series of dilatometer tests were performed and the start/end temperatures of each phase transformation were measured for wide range of constant cooling rates. Information of phase volume fractions were obtained from microsections analysis after samples cooling to room temperature. Hence, the problem of parameters estimation can be transformed to the optimization task:

$$\Phi(\mathbf{a}) = \left\| \mathbf{y}(\mathbf{a}) - \mathbf{y} \right\|^2 \tag{26}$$

where $\mathbf{y}(\mathbf{a})$ is the model output vector, $\mathbf{y}$ is measured vector.

It can be proved (Kirsch, 1996) that minimum of the goal function (26) is the solution of the inverse problem (25).

Basic principles of the inverse method were described in a number of publications, see for example (Szeliga et al., 2006). The most frequent applications of the inverse method in metallurgy were connected with determination of coefficients in flow stress models of materials subjected to plastic deformation, see e.g. Szeliga et al. (2006), Forestier et al. (2002). Applications of the inverse approach to the identification of the phase transformation model on the basis of the constant cooling rate dilatometric tests were less frequent. Some of the investigations were presented in Pietrzyk et al. (2003).

Identification of the phase transformation JMAK model parameters $\mathbf{a} = \{a_1 \ldots a_{30}\}$ was performed with the goal function defined as (26), which in the particular case of phase transformations is of the form:

$$\Phi(\mathbf{a}) = \sqrt{\frac{1}{n}\sum_{i=1}^{n}\left(\frac{T_i^m - T_i^c(\mathbf{a})}{T_i^m}\right)^2 + \frac{1}{l}\sum_{i=1}^{l}\left(\frac{X_i^m - X_i^c(\mathbf{a})}{X_i^m}\right)^2} \tag{27}$$

where: T_i^m, $T_i^c(\mathbf{a})$ – measured and calculated start and end temperatures of phase transformations, n – number of temperature measurements, X_i^m, $X_i^c(\mathbf{a})$ – measured and calculated phases volume fractions at room temperature, l – number of measurements of phases volume fractions.

The values of the $\mathbf{a}$ parameters obtained from the inverse analysis were given in table 4. The whole JMAK model for all transformations contains 30 parameters, see section 2.1. However, after simplification based on the sensitivity analysis only 26 of them were active in the transformation model for the considered DP steel and were used in the present work. Model described by parameters presented in table 4 was validated. It was used to simulate all performed dilatometer tests. Figure 6a shows comparison of the measured (filled symbols) and predicted (open symbols) start and end temperatures for the phase transformations. Shape of the symbol refers to the temperature in the legend. Analysis of the results confirms that the model predicts quite well start and end temperatures for transformations, although the accuracy is slightly worse for the pearlite start and bainite end temperatures. Figure 6b shows calculated volume fractions of phases.

Phase transformation model with the estimated parameters was implemented in the FE code and it was used in simulations of two case studies presented in the next chapter.

Table 4. *Coefficients in the phase transformation model calculated using inverse analysis for the investigated DP steel.*

a_1	a_2	a_3	a_4	a_5	a_6	a_7	a_8	a_9
1039	4.861	2.866	1.333	0.673	157.9	39.83	1.983	64.76
a_{10}	a_{11}	a_{12}	a_{15}	a_{17}	a_{18}	a_{19}	a_{20}	a_{21}
1.106	0.618	0.153	1.285	1842	66.59	3.489	692.7	0.181
a_{22}	a_{23}	a_{24}	a_{25}	a_{25}	a_{26}	a_{28}	a_{29}	a_{30}
0.074	0.406	1.049	435.8	0	1.732	9636	79.4	0.229

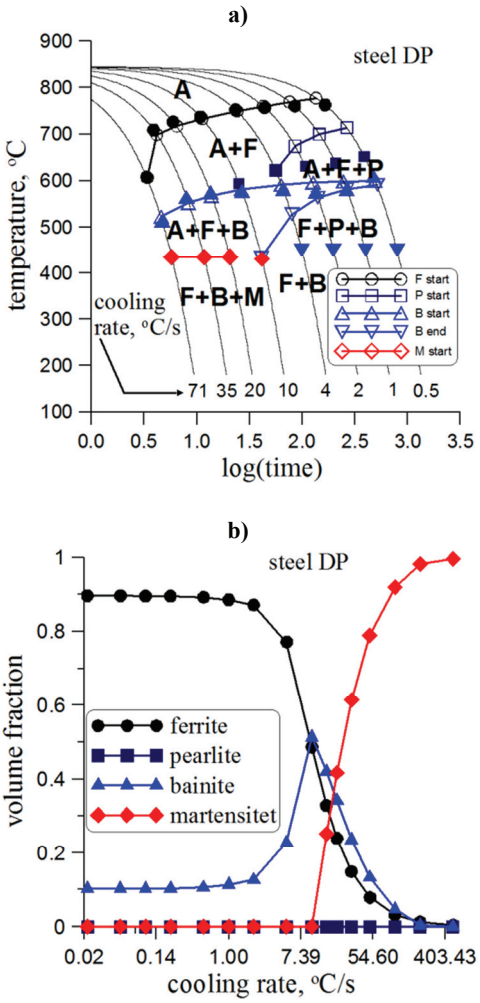

Fig. 6. Comparison of the predictions of the optimized phase transformation model (coefficients in tables 6 and 7) with measurements for the transformations start and end temperatures (a) and for volume fractions of phases (b).

4. CASE STUDIES

Two processes were selected as the case studies for testing the modified JMAK model. The first was cooling with various cooling rates of samples after multi step hot forming. Physical simulations of this process were performed to validate the model. Continuous annealing after cold rolling was selected as the second case study in the present work.

4.1. Cooling after multi step hot forming

The objective of the experiment was to reproduce hot rolling followed by accelerated cooling for the DP steel. The experiment was performed on the Gleeble 3800 at the Institute for Ferrous Metallurgy in Gliwice. Scheme of the experiment is shown in figure 7. The samples were preheated at 1200°C for 20 s, cooled to 1180°C and deformed at 7 stages of plane strain compression with strains of 0.2/0.2/0.25/0.25/0.25/0.25/0.3 at decreasing temperatures. The last deformation was performed at 870°C. Accelerated cooling followed with the cooling rates of 4.5°C/s; 5°C/s and 5.5°C/s to the temperature 610°C. All the samples were quenched in water after that. The cooling rates after hot deformation were selected to reproduce industrial processes of manufacturing of DP steels, which contain about 20-30% of martensite.

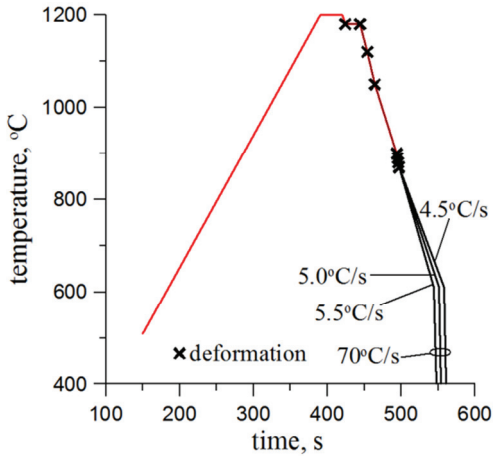

Fig. 7. Scheme of the multi step hot deformation followed by accelerated cooling.

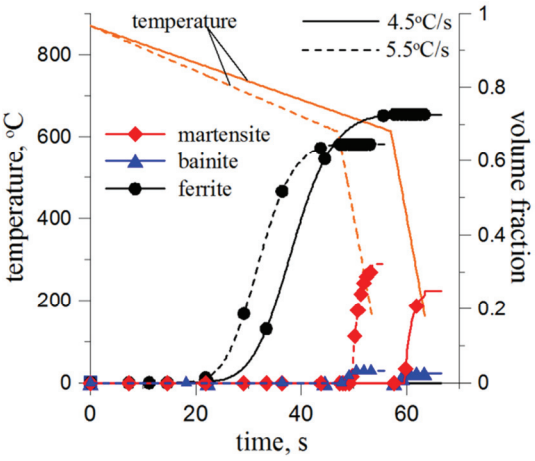

Fig. 8. Scheme of the multi step hot deformation followed by accelerated cooling.

Simulation of microstructure evolution during hot deformation gave the final austenite grain size of 19 μm. Since this work is focused on modelling phase transformations after hot deformation, the microstructure evolution models during hot forming were not described here, they can be found in Pietrzyk and Kuziak (2011). Results of simulation of cooling after hot deformation for two cooling rates (4.5°C/s and 5.5°C/s) were shown in figure 8.

Microstructure of the samples after processing was investigated and main parameters were quantitatively estimated. Measured volume fraction of the martensite was used for validation of the model in figure 9.

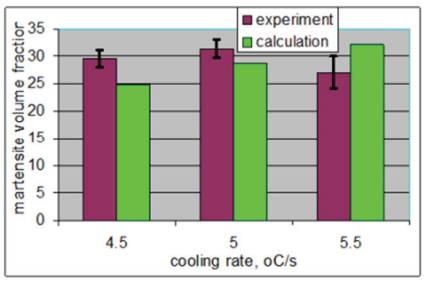

Fig. 9. Measured and calculated volume fraction of martensite for different cooling rates after deformation.

4.2. Continuous annealing

Simulations of the continuous annealing after cold rolling were performed to test the predictive capabilities of the model. Four thermal profiles characteristic for the continuous annealing were considered. Schematic illustration of the typical continuous annealing thermal cycle is shown in figure 10a and the investigated cycles were shown in figure 10b. Heating/cooling rates, as well as the end temperature for each part of the cycle were the controllable parameters of the cycle. The values of these parameters were given in table 5. In the last part of each cycle C_{r5} was 20°C/s and the end temperature was equal to the room temperature. The sensitivity analysis of the continuous annealing model with respect to the controllable parameters of the cycle was presented by Szeliga (2012b).

Table 5. *Heating/cooling rates [°C/s] and end temperatures [°C] for each part of the thermal cycles for the investigated annealing processes.*

cycle	H_{r1}	T_{h1}	H_{r2}	T_{h2}	C_{r1}	T_{c1}	C_{r2}	T_{c2}	C_{r3}	T_{c3}	C_{r4}	T_{c4}
A1	3	755	0.25	765	10	710	1.5	700	40	350	0.6	320
A2	3	880	0.25	890	10	710	1.5	700	40	350	0.6	320
A3	3	780	0.25	790	10	710	1.5	700	15	350	0.6	320
A4	3	780	0.25	790	10	710	1.5	700	60	350	0.6	320
A5	3	780	0.25	790	10	710	1.5	696	60	350	0.6	320

Results of simulations of the annealing thermal cycles A1-A4 in table 5 were presented in figures 11 and 12. Changes of volume fractions of phases were presented in figures 11a and 11a. Thermal cycles A1 and A2 differed by the maximum temperature of the cycle. This temperature was 890°C for the case A2 and full austenitization after heating was obtained. The maximum temperature in the case A1 was 765°C, which was in the lower part of the intercritical region. In consequence, over 70% of ferrite remained in the microstructure after heating. The cases A3 and A4 represent annealing in the inter critical region of temperature but with the maximum temperature of 790°C, which is higher than in the case A2. The difference between A3 and A4 was in the cooling rate during fast cooling (C_{r3} = 15°C/s and 60°C/s respectively).

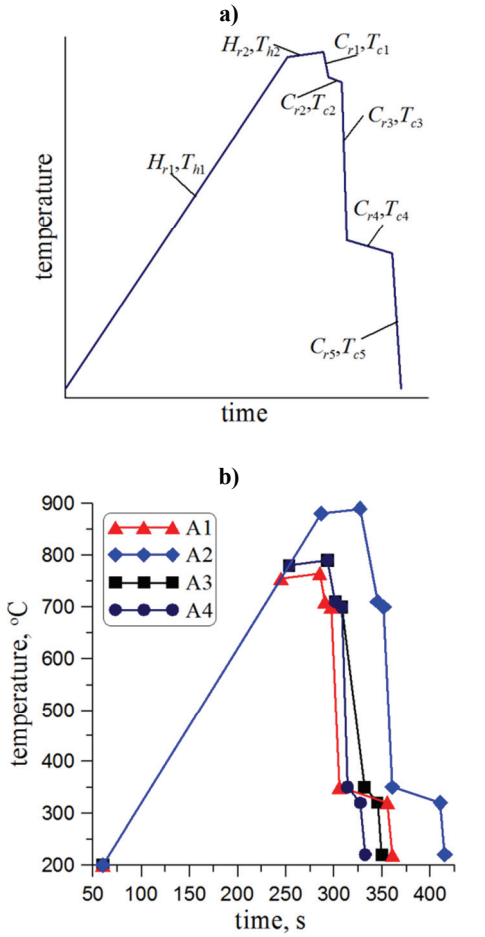

Fig. 10. A typical continuous annealing thermal profile (a) and thermal profiles for annealing processes investigated in this work (b).

Changes of the average carbon concentration in the austenite were presented in figures 11b and 12b. It is seen in this figure that the largest carbon concentration was obtained for the case A1, in which final volume fraction of the ferrite was the largest.

Volume fractions of phases after various annealing cycles were shown in figure 13. It is seen in this figure that the required volume fraction of the ferrite at the level of 0.7 was obtained for the case A3, but the disadvantageous excess of the bainite over the martensite was observed. The volume fraction of the ferrite was slightly too low in the case A4, but only negligible amount of the bainite was obtained in that case. On the basis of these simulations and the sensitivity analysis performed by Szeliga (2012b) it was easy to deduce that slight increase of the slow cooling time t_{c2} will allow to obtain required volume fraction of the martensite around 0.25 with the negligible amount of the bainite. The parameters of this case were given as A5 in table 5 and in figure 13.

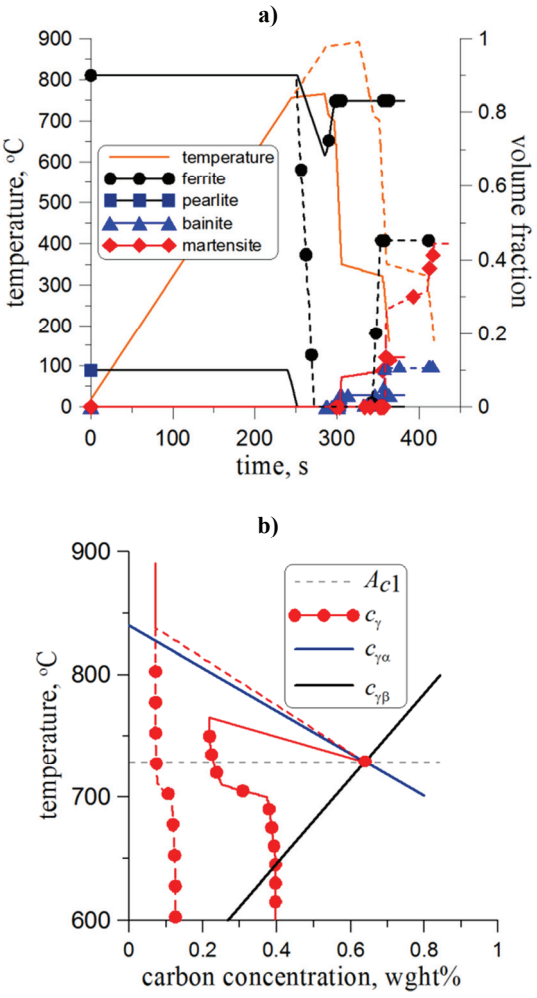

***Fig. 11**. a) Temperature and kinetics of transformations during annealing cycles A1 (solid lines) and A2 (dotted lines) b) Changes of the average carbon concentration in the austenite during annealing cycles A1 (solid line) and A2 (dotted line).*

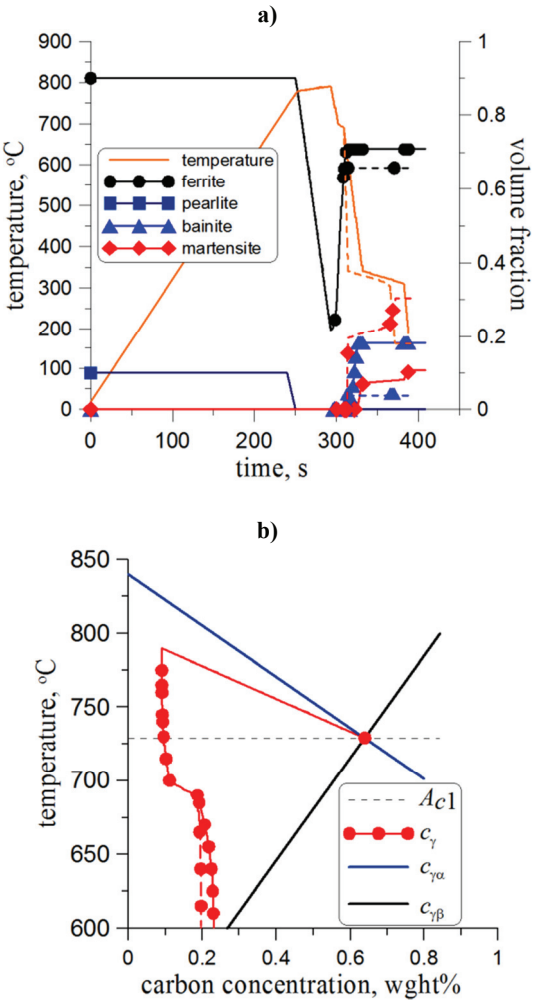

***Fig. 12.** a) Temperature and kinetics of transformations during annealing cycles A3 (solid lines) and A4 (dotted lines) b) Changes of the average carbon concentration in the austenite during annealing cycles A3 (solid line) and A4 (dotted line).*

5. CONCLUSIONS

Critical analysis and identification of phase transformation models for steel was performed in the paper. The following observations were made:

- The model based on the modified JMAK equation is an efficient and satisfactorily accurate and it can be used for optimization of manufacturing of DP steels when volume fraction of phases are the objectives of the optimization.
- Sensitivity analysis allowed to simplify the modified JMAK equation model by removing relation of the temperature coefficient describing kinetics of the pearlite transformation.
- Case studies for physical models of laminar cooling and continuous annealing confirmed good predictive capabilities of the model.

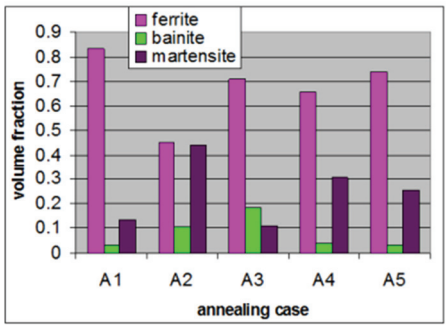

***Fig. 13.** Volume fractions of phases after various annealing cycles.*

ACKNOWLEDGEMENTS

Financial assistance of the NCN, project N N508 629 740, is acknowledged.

REFERENCES

Avrami, M., 1939, Kinetics of phase change I, *J. Chem. Phys.*, 7, 1103-1112.

Bhadeshia. H.K.D.H., 2001, *Bainite in steels*, University Press, Cambridge.

Donnay, B., Herman, J.C., Leroy, V., Lotter, U., Grossterlinden, R., Pircher, H., 1996, Microstructure evolution of C-Mn steels in the hot deformation process: the STRIPCAM model, *Proc. 2nd Conf. Modelling of Metal Rolling Processes*, eds. Beynon, J.H., Ingham, P., Teichert, H., Waterson, K., London, 23-35.

Forestier, R., Massoni, E., Chastel, Y., 2002, Estimation of constitutive parameters using an inverse method coupled to a 3D finite element software, *Journal of Materials Processing Technology*, 125, 594-601.

Johnson, W., Mehl, R., 1939, Reaction kinetics in processes of nucleation and growth, *Trans. AIME*, 135, 416-58.

Kirsch, A., 1996, *An Introduction to the Mathematical Theory of Inverse Problems*, Springer.

Kleiber, M., Antunez, H., Hien, T.D., Kowalczyk, P., 1997, *Parameter Sensitivity in Nonlinear Mechanics*, Wiley.

Koistinen, D.P., Marburger, R.E., 1959, A general equation prescribing the extent of the austenite-martensite transformation in pure iron-carbon alloys and plain carbon steels, *Acta Metallurgica*, 7, 59-60.

Kolmogorov, A., 1937, K statisticheskoi teorii kristallizatsii metallov, *Izv. Akad. Nauk USSR Ser. Matemat.*, 3, 355-59.

Kondek, T., Kuziak, R., Pietrzyk, M., 2003, Finite Element Modelling of Deformation of Steels in Two-Phase Range of Temperatures, *Proc. COMPLAS VII*, eds. Owen, D.R.J., Onate, E., Suarez, B., CIMNE, Barcelona, CD ROM.

Lan, Y.J., Li, D.Z., Li, Y.Y., 2004, Modeling austenite decomposition into ferrite at different cooling rate in low-carbon steel with cellular automaton method, *Acta Materialia*, 52, 1721-1729.

McKay, M.D., 1995, Evaluating prediction uncertainty, *Technical Report NUREG/CR-6311*, U.S. Nuclear Regulatory Commission and Los Alamos National Laboratory.

McKay, M.D., Conover, W.J., Beckman, R.J., 1979, A comparison of three methods for selecting values of input variables in the analysis of output from a computer code, *Technometrics*, 21, 239-245.

Mecozzi, M.G., Militzer, M., Sietsma, J., van Der Zwaag, S., 2008, The role of nucleation behavior in phase-field simulations of the austenite to ferrite transformation, *Metallurgical and Materials Transactions A*, 39A, 1237-1247.

Militzer, M., 2011, Phase field modeling of microstructure evolution in steels, *Current Opinion in Solid State and Materials Science*, 15, 106-115.

Morris, M.D., 1991, Factorial sampling plans for preliminary computational experiments. *Technometrics*, 33, 161-174.

Pernach, M., Pietrzyk, M., 2008, Numerical solution of the diffusion equation with moving boundary applied to modeling of the austenite-ferrite phase transformation, *Computational Materials Science*, 44, 783-791.

Pietrzyk, M., Kuziak, R., 1999, Coupling the thermal-mechanical finite-element approach with phase transformation model for low carbon steels, *Proc. 2nd ESAFORM Conf. on Material Forming*, ed., Covas J., Guimaraes, 525-528.

Pietrzyk, M., Kuziak, R., Kondek, T., 2003, Physical and numerical modelling of plastic deformation of steels in two-phase region, *Proc. 45th MWSP Conf.*, Chicago, 209-220.

Scheil, E., 1935, Anlaufzeit der Austenitumwandlung, *Archiv. für Eissenhüttenwesen*, 12, 565-567.

Simmons, J.P., Shen, C., Wang, Y., 2000, Phase field modeling of simultaneous nucleation and growth by explicitly incorporating nucleation events, *Scripta Materialia*, 43, 935-942.

Sobol' , I.M., 1993, Sensitivity analysis for non linear mathematical models, *Math. Model. Comput. Exp.*, 1, 407 – 414.

Suehiro, M., Senuma, T., Yada, H., Sato, K., 1992, Application of mathematical model for predicting microstructural evolution to high carbon steels, *ISIJ International*, 32, 433-439.

Szeliga, D., Gawąd, J., Pietrzyk, M., 2006, Inverse analysis for identification of rheological and friction models in metal forming, *Computer Methods in Applied Mechanics and Engineering*, 195, 6778-6798.

Szeliga, D., Pietrzyk, M., 2010, Identification of rheological models and boundary conditions in metal forming, *International Journal of Materials and Product Technology*, 39, 388- 405.

Szeliga, D., 2011, Application of sensitivity analysis – preliminary step of the process parameters estimation. *Proc. XI Conf. COMPLAS*, eds. Oñate, E., Owen, D.R.J., Peric, D., Suarez, B., Barcelona, 1359-1367, (e-book).

Szeliga, D., Pietrzyk, M., 2011, Multiscale models and metamodels in application to metal forming simulations, *Proc. MEFORM 2011*, Freiberg, 364-369.

Szeliga, D., 2012a, Zagadnienie identyfikacji parametrów równań przemian fazowych, *Rudy i Metale Nieżelazne*, 57, (in press) (in Polish).

Szeliga, D., 2012b, Design of the continuous annealing process for multiphase steel sheets, *Proc. Conf METAL 2012*, Brno, (CD ROM).

Tamura, I., Ouchi, C., Tanaka, T., Sekine, H., 1988, *Thermomechanical processing of high strength low alloy steels*, Butterworth & Co. Press, London.

Umemoto, M., Hiramatsu, A., Moriya, A., Watanabe, T., Nanba, S., Nakajima, N., Anan, G., Higo, Y., 1992, Computer modelling of phase transformation from work-hardened austenite, *ISIJ International*, 32, 306-315.

van Leeuwen, Y., Kop, T.A., Sietsma, J., van der Zwaag, S., 1999, Phase transformations in low-carbon steels; modelling the kinetics in terms of the interface mobility, *Journal of Physics IV*, 9, 401-09.

Zhang, L., Zhang, C.B., Wang, Y.M., Wang, S.Q., Ye, H.Q., 2003, A cellular automaton investigation of the transformation from austenite to ferrite during continuous cooling, *Acta Materialia*, 51, 5519-5527.

Zienkiewicz, O.C., Taylor, R.L., 1989, *The Finite element method*, McGraw-Hill.

DOBÓR MODELU PRZEMIAN FAZOWYCH DLA PROCESU LAMINARNEGO CHŁODZENIA I WYŻARZANIA STALI DWUFAZOWYCH

Streszczenie

W pracy przedstawiono zmodyfikowany model przemian fazowych oparty na równaniu JMAK, umożliwiający modelowanie procesu laminarnego chłodzenia i wyżarzania stali dwufazowych. Dla modelu przemian wyznaczono jego najistotniejsze parametry korzystając z metod analizy wrażliwości. Następnie wyznaczono parametry modelu przemian dla stali dwufazowej. Zagadnienie identyfikacji parametrów modelu zdefiniowano jako zadanie odwrotne korzystając z wcześniejszych wyników analizy wrażliwości. Ilościowe oszacowanie parametrów zostało zweryfikowane na podstawie pomiarów dylatometrycznych oraz analizy obrazów mikrostruktury. W drugiej części pracy zaprezentowano obliczenia dla dwóch różnych procesów przemysłowych z wykorzystaniem modelu przemian fazowych połączonym z metodą elementów skończonych. Otrzymane wyniki potwierdziły przydatność opracowanych modeli do modelowania złożonych procesów przemysłowych łączących formowanie materiału z procesem chłodzenia bądź wyżarzania.

Received: July 11, 2012
Received in a revised form: July 24, 2012
Accepted: August 09, 2012